Int J Thermophys (2018) 39:33
https://doi.org/10.1007/s10765-017-2356-x

ICPPP 19

Photopyroelectric Calorimetry Investigations of 8CB Liquid Crystal–Microemulsion System

S. Paoloni[1] · **U. Zammit**[1] · **F. Mercuri**[1]

Received: 20 September 2017 / Accepted: 30 December 2017 / Published online: 12 January 2018
© Springer Science+Business Media, LLC, part of Springer Nature 2018

Abstract In this work, the photopyroelectric technique has been used to investigate the phase transitions in a liquid crystal microemulsion by combining the simultaneous high temperature resolution thermal diffusivity measurements and optical polarization microscopy observations. It has been found that, during the conversion from the isotropic phase into the nematic one, the micelles are expelled from the nematic domains and remain confined in islands of isotropic material which survive down to the smectic temperature range. A hysteresis in the thermal diffusivity profiles between heating and cooling run over the isotropic–nematic transition temperature range has been observed which has been ascribed to the different micelles distribution into the sample volume during cooling and heating runs. Finally, the almost bulk-like behavior of the thermal diffusivity over the nematic–smectic phase transition confirms that a significant fraction of the micelles are expelled during the nucleation of the nematic phase.

Keywords Calorimetry · Liquid crystals · Microemulsions · Phase transitions

1 Introduction

Liquid crystal microemulsions (LCM) composed of dispersed didodecyl-dimethyl-ammonium bromide (DDAB) surfactant-coated water droplets (inverse micelles) in a

This article is part of the selected papers presented at the 19th International Conference on Photoacoustic and Photothermal Phenomena.

✉ S. Paoloni
stefano.paoloni@uniroma2.it

[1] Dipartimento di Ingegneria Industriale, Università degli Studi di Roma "Tor Vergata", Via del Politecnico 1, 00133 Rome, Italy

liquid crystal (LC) host have been intensively studied [1–6] due to their peculiar physical properties arising from the inter-micelles interaction mediated by the anisotropic ordering of the LC host.

Previous measurements had been taken in 8CB-LCM samples consisting of micelles dispersed into 4-octyl-4-cyanobiphenyl (8CB) LC [7]. In particular, the relaxation calorimetry [8] had been adopted to measure the release of latent heat associated with the isotropic (I)–nematic (N) first-order phase transition. Unlike pure 8CB LC, where the latent heat is released over a very narrow temperature range around the phase transition temperature T_{NI}, in 8CB-LCM samples such a release has been found to occur over the whole N temperature range and, for large micelle concentration, even down to the smectic (A) one. This clearly indicated that, in 8CB- LCM, the nucleation of the N phase from the I one takes place over a wide temperature range. Such a result had been interpreted as follows [9–12]. The presence of the dispersed micelles leads to a weakening of the interaction strength between LC molecules and, consequently, to a decrease of the T_{NI} value with respect to the pure 8CB LC one. Therefore, upon cooling from the I phase, in 8CB-LCM the beginning of the N phase nucleation does not occur uniformly over the sample volume but it starts at the sample positions where the micelles concentration is lowest. In addition, since in the newly formed N domains the LC molecules are forced to align orthogonally to the micelles surface by the presence of the DDAB surfactant, the nematic director becomes locally distorted by the randomly distributed micelles. In order to release the extra elastic energy cost associated with such a molecular arrangement, the micelles are continuously expelled from the nucleating N domains and remain confined into sample regions where the micelles concentration becomes larger, with correspondingly lower values of T_{NI}. Therefore, an inhomogeneous medium is produced composed of coexisting N domains and islands of residual micelles-rich I phase. Upon cooling, latent heat is released over a large temperature range because of the continuous occurrence of the first-order transition converting super-cooled I regions into new N domains.

Ac calorimetry had also been applied to measure the specific heat temperature dependence in the 8CB-LCM samples [7]. In comparison with pure 8CB LC, the specific heat peak corresponding to the IN phase transition had been found to be broadened and shifted to lower temperature by the presence of micelles. Moreover, significant hysteresis had been observed between the specific heat profiles over the N range obtained in subsequent heating and cooling runs, the specific heat features during the heating runs having been obtained at larger temperature with respect to the corresponding ones observed during the cooling runs. A justification for these results could be given following nuclear magnetic resonance (NMR) and optical observations [12]. Briefly, it had been found that, during the cooling runs, the coexisting N and micelles-rich I phases are vertically separated by gravity due to their different mass density. Moreover, the nematic material turning isotropic during the heating run had a considerably lower micelles content with respect to the cooling run so that the corresponding peaks of the specific heat profile were shifted to larger temperature values with respect to those corresponding to the cooling runs.

In the present work, we investigate the phase transitions in thin 8CB-LCM samples, since, because of the very limited thickness preventing the separation between N and I phases to be affected by gravity [7–12], other mechanisms involved in the

phase separation and in the micelles migration can be studied. The study was carried out by the high temperature resolution thermal diffusivity measurements and optical polarization microscopy observations, simultaneously carried out in a photopyroelectric (PPE) calorimetric setup [13–18], so that the different kind of data are obtained from the same sample under the same experimental conditions [19–22]. This allows to perform accurate cross-correlation of the results concerning the different measured quantities. Like other photothermal techniques [23–29], PPE can be used for the characterization of the thermophysical parameters in liquids and solids. In the present work, the thermal diffusivity was considered for the sample characterization over the phase transitions since, on the one hand, the detected minima reflect the peaks pertaining to the specific heat and they are useful to identify the phase transition temperatures. On the other hand, its absolute values in the mesophases are dependent on the degree of molecular alignment, as it occurs for the thermal conductivity, and they are thus useful to probe the degree of homeotropic alignment of the LC molecules.

2 Experimental Results and Discussion

The investigated 8CB-LCM samples were prepared according to the procedure described in Ref. [7] where three different weight fractions, $\Phi = 0.03$, 0.06 and 0.12, of DDAB and water mixtures (weight ratio $m(DDAB)/[m(DDAB) + m(H_20)] = 0.85$), have been dissolved into pure 8CB LC.

In the present investigations, the back detection configuration of the PPE technique has been adopted whose detailed description is reported elsewhere [15]. The measurements were taken in a 30-μm-thick sample cell. In the adopted PPE configuration, the Ti-coated side of the sample cell is heated by a modulated laser beam in order to generate a thermal wave which, after diffusing through the sample, is detected at the opposite side by a 300-μm-thick Z-cut LiTaO3 pyroelectric crystal. The sensor output signal is then analyzed by means of appropriate theoretical expressions which enables the determination of the thermal parameters, among which the thermal diffusivity D. Thanks to the transparency of the pyroelectric transducer and of the adopted Indium Tin Oxide electrodes, a linearly polarized white light beam can be conveyed through the sample and, after the reflection form the previously mentioned metallic coating, it is directed onto a CCD camera. In this way, the PPE calorimetric setup allows to monitor also the sample morphology during the thermal parameters measurements thanks to the simultaneously performed polarization microscopy observation.

In Fig. 1, the thermal diffusivity results obtained in pure 8CB are shown, while in Fig. 2a the results obtained in a 8CB-LCM sample ($\Phi = 0.03$) during a cooling and a subsequent heating runs are reported. With respect to the pure material, the minima in the 8CB-LCM thermal diffusivity profiles corresponding to the NI phase transition are broadened by the presence of the micelles and shifted to lower temperature values. As already found in the previous *ac* calorimetry investigations [7] and in more recent PPE thermal conductivity and specific heat measurements [30], a significant hysteresis can be observed also in the thermal diffusivity profiles between heating and cooling runs, the minimum over the NI phase transition observed during the heating run being shifted to higher temperature value in comparison with that obtained during the cooling run.

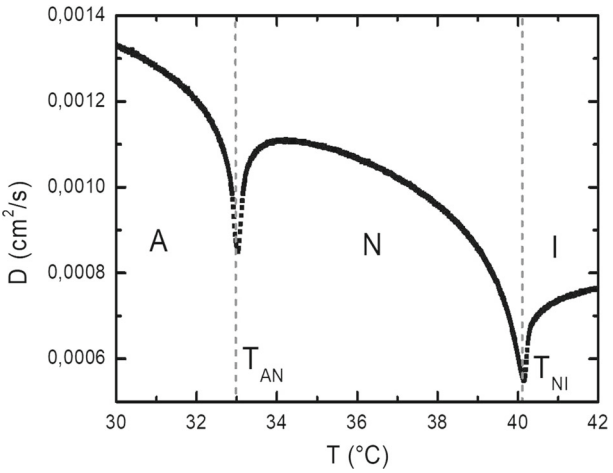

Fig. 1 Thermal diffusivity profile over the smectic A–isotropic I range in pure homeotropic 8CB LC sample

On the contrary, an almost bulk-like sharp profile of the dip over the nematic–smectic transition temperature T_{NA} has been found where a less evident hysteresis can also be observed between heating and cooling run. Finally, the thermal diffusivity values are very similar to the ones obtained with the pure 8CB sample, particularly in the smectic phase. In this respect, it is worth to note that the measurements in the pure 8CB sample have been obtained in a sample cell whose walls had been treated with surfactant in order to promote the LC molecules orientation orthogonal to the cell walls (homeotropic alignment) and, hence, parallel to the heat flux. Since the 8CB thermal diffusivity is an anisotropic property, with the D value along the main molecular axis approximately three times larger than the orthogonal one [31], the above-mentioned similarity in the D values in the A phase implies a similar degree of homeotropic alignment in the pure sample and in that with micelles.

In Fig. 2, the thermal diffusivity profiles obtained for the other two micelles concentrations, namely $\Phi = 0.06$ (Fig. 2b) and 0.12 (Fig. 2c), are reported. The comparison of these results with the ones obtained in the $\Phi = 0.03$ sample shows that during the cooling runs the T_{NI} transition temperature is progressively shifted downward for increasing micelles concentration. On the contrary, the T_{NI} values corresponding to the heating runs are very similar regardless of the Φ value. As for the NA phase transition, the T_{NA} values and the thermal diffusivity minima over such a temperature range are, at least in the investigated Φ range, almost independent on the micelles concentration. This confirms that the N material is well refined from micelles before it turns into the A phase. In addition, a small hysteresis can be observed, being both the T_{NA} values and the extent of the D variations larger during the heating runs.

An explanation for these results could be proposed thanks to the simultaneously performed polarization microscopy observations. Upon cooling from the I phase, the nucleation of the first N domains begins at one of the sample cell walls and, when they get to touch both walls, they align homeotropically with I material all around.

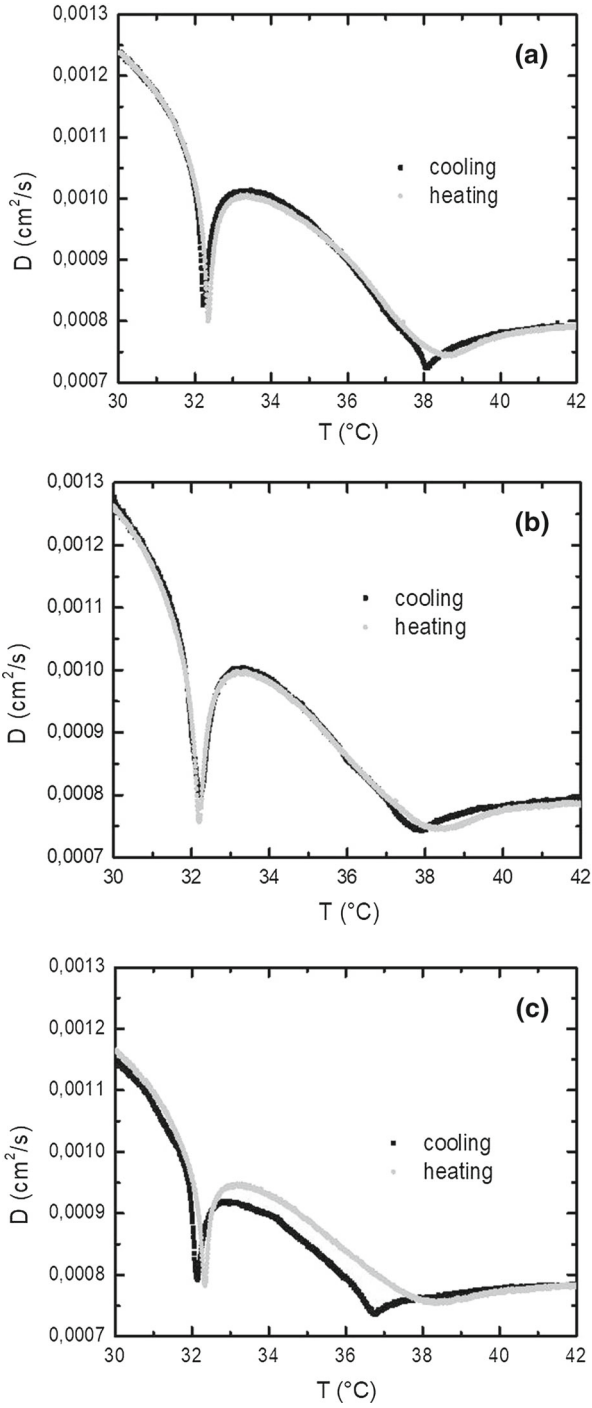

Fig. 2 Thermal diffusivity profiles in 8CB-LCM with $\Phi = 0.03$ (a), $\Phi = 0.06$ (b) and $\Phi = 0.12$ (c) sample during cooling (black)and subsequent heating (gray)

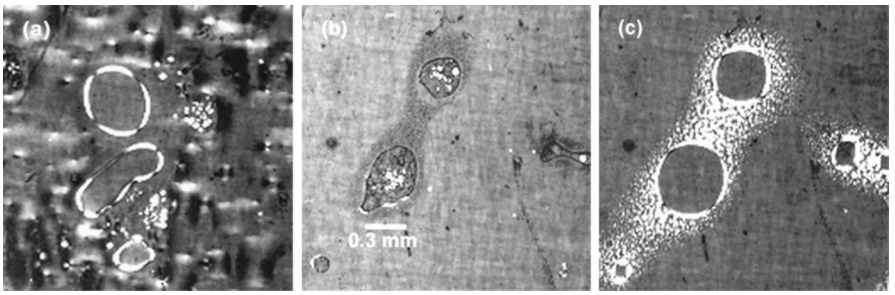

Fig. 3 Polarization microscopy images taken on the same area in 8CB-LCM sample with $\Phi = 0.06$ during cooling at T = 36.8 °C (a); T = 31.2 °C (b) and during subsequent heating at T = 37.5 °C (c)

The homeotropic alignment is achieved since part of the DDAB surfactant used to produce the micelles is deposited at the cell walls where it acts as an aligning agent for the nematic domains. As shown in Fig. 3a, the homeotropic N domains appear as uniform dark areas bounded by birefringent borders, where the LC molecules alignment deviates from the homeotropic one, and they are surrounded by non-birefringent I material.

Upon further cooling, the N domains grow in number and size until islands of isotropic materials remain, having a large concentration of micelles due to their progressive expulsion from the nucleating N domains. In this respect, it is worth reminding that in the several mm thick samples the micelles migration occurred vertically through the horizontal interface between the separated N and I phase [12]. On the contrary, the present results indicated that in thin samples the micelles expulsion toward the residual I islands occur in the horizontal plane through the N domains limiting surfaces. Therefore, an accumulation of micelles in the N material areas nearest the interface with the isotropic volumes is expected. As shown in Fig. 3b, when all the N material outside the micelles-rich I islands has turned smectic, a network of fine grained defects appears only around the border of the I islands confirming that these smectic areas posses a larger micelles concentration with respect to the ones further away from the islands. Such finding is consistent with the sharp dip shown by D over the NA transition since most of the nematic material turning smectic is almost depleted of micelles. In addition, the small hysteresis observed in the D profiles between heating and cooling runs over NA transition supports the idea that, over such a transition, an additional reduction in the micelles content in the final smectic phase is obtained with respect to that having already occurred during the I–N conversion. Finally, it must be pointed out that the lighter areas appearing within the I micelles-rich islands correspond to birefringent N domains still surviving down to the smectic temperature range because of their relatively large micelle content.

Upon heating form the smectic phase, the order of events is reversed with respect to what occurred during the cooling run. The defects around the I islands become visible again and those are the areas which turn nematic at the lowest temperature because of their corresponding larger micelle concentration. Upon further heating, the size of the I islands starts to increase since the N material close to their borders begins to convert into the I phase. There are also areas where the N material starts

melting to isotropic which correspond to the bright spots observed in Fig. 3c. In fact, the presence of isotropic material detaches the N domains from one of the cell walls, thus destroying their homeotropic alignment and making them birefringent again. Owing to the micelles separation process occurred during the cooling run, the nematic material turning isotropic during the heating run has a much lower micelles content than the isotropic material turning nematic in the cooling run. Therefore, the T_{NI} transition temperature is shifted to larger values with respect to those observed during the cooling run. In this respect, the similarity of the T_{NI} values obtained during the heating runs for all the samples can be ascribed to a common micelles content which had been retained, during the previous cooling run, in the nucleating nematic and smectic material, irrespective of the initial micelle concentration. Finally, upon further heating the melting to the isotropic phase progresses until all the material becomes isotropic.

3 Conclusions

In this work, we have used a PPE setup to analyze the phase transitions in 30 μm thick 8CB-LCM samples by combining the thermal diffusivity measurements with the simultaneously performed polarization microscopy observations. This kind approach has proven to be very effective for the investigation of phase transitions thanks to the possibility to combine different kinds of simultaneous measurements, on the same sample, under the same experimental conditions.

It was found that, upon cooling from the I phase, the micelles are progressively expelled from the nucleated N domains and remain confined within islands of residual I material which can survive down to temperature values corresponding to the smectic range. Unlike the case of thick samples, where the micelles migration occurs through the horizontal interface between the gravity-separated N and I phase, in thin samples the migration is shown to occur through the nematic domains lateral limiting surface.

A hysteretic behavior has been observed in the thermal diffusivity profiles over the NI phase transition temperature range because of the larger micelles content in the isotropic material turning nematic during the cooling run with respect to the nematic turning isotropic in the subsequent heating run.

Finally, the almost bulk-like dip of the thermal diffusivity over the NA phase transition indicates that a significant number of micelles are expelled during the nucleation of the nematic phase and, therefore, almost micelles-free N phase undergoes the phase conversion into the A phase. In addition, a small hysteresis has been observed also over the NA transition reflecting a further micelles expulsion occurring as the sample cools from the N to the A phase.

References

1. P. Poulin, H. Stark, T. Lubensky, D. Weitz, Science **275**, 1770 (1997)
2. J.C. Loudet, P. Barois, P. Poulin, Nature **407**, 611 (2000)
3. G. Toquer, G. Porte, M. Nobili, J. Appell, C. Blanc, Langmuir **23**, 4081 (2007)
4. J. Yamamoto, H. Tanaka, Nature **409**, 321 (2001)
5. Z. Chen, R. Nozaki, J. Chem. Phys. **134**, 034505 (2011)

6. Z. Chen, R. Nozaki, Phys. Rev. E **84**, 011401 (2011)
7. Z. Kutnjak, G. Cordoyiannis, G. Nounesis, A. Lebar, B. Zalar, S. Zumer, J. Chem. Phys. **122**, 224709 (2005)
8. H. Yao, K. Ema, C.W. Garland, Rev. Sci. Instrum. **69**, 173 (1998)
9. T. Bellini, M. Caggioni, N.A. Clark, F. Mantegazza, A. Maritan, A. Pellizzola, Phys. Rev. Lett. **91**, 085704 (2003)
10. M. Caggioni, A. Giacometti, T. Bellini, N.A. Clark, F. Mantegazza, A. Maritan, J. Chem. Phys. **122**, 214721 (2005)
11. R. Pizzoferrato, T. Ziller, A. Micozzi, A. Ricci, C. Lo Sterzo, A. Ustione, C. Oliva, A. Cricenti, Chem. Phys. Lett. **414**, 234 (2005)
12. A. Lebar, Z. Kutnjak, H. Tanaka, B. Zalar, S. Zumer, Phys. Rev. E **78**, 031707 (2008)
13. A. Mandelis, M. Zver, J. Appl. Phys. **57**, 4421 (1985)
14. M. Massot, A. Oleaga, A. Salazar, D. Prabhakaran, M. Martin, P. Berthet, G. Dhalenne, Phys. Rev. B **77**, 134438 (2008)
15. U. Zammit, M. Marinelli, F. Mercuri, S. Paoloni, F. Scudieri, Rev. Sci. Instrum. **82**, 121101 (2011)
16. J. Caerels, C. Glorieux, J. Thoen, Phys. Rev. E **65**, 031704 (2002)
17. U. Zammit, M. Marinelli, F. Mercuri, S. Paoloni, J. Phys. Chem. B **113**, 14315–14322 (2009)
18. U. Zammit, M. Marinelli, F. Mercuri, S. Paoloni, F. Scudieri, J. Phys. Chem. B **115**, 2331 (2011)
19. S. Paoloni, F. Mercuri, M. Marinelli, U. Zammit, C. Neamtu, D. Dadarlat, Phys. Rev. E **78**, 042701 (2008)
20. U. Zammit, S. Paoloni, F. Mercuri, M. Marinelli, F. Scudieri, AIP Adv. **2**, 012135 (2012)
21. D. Dadarlat, C. Neamtu, R. Pop, M. Marinelli, F. Mercuri, J. Optoelectron. Adv. Mater. **9**, 2847 (2007)
22. U. Zammit, F. Mercuri, S. Paoloni, M. Marinelli, R. Pizzoferrato, J. Appl. Phys. **117**, 105104 (2015)
23. J.A. Balderas-Lòpez, A. Mandelis, Rev. Sci. Instrum. **74**, 5219 (2003)
24. M. Kuriakose, M. Depriester, D. Dadarlat, A.Hadj Sahraoui, Meas. Sci. Technol. **24**, 025603 (2013)
25. A. Salazar, A. Oleaga, Rev. Sci. Instrum. **83**, 014903 (2012)
26. F. Mercuri, S. Paoloni, N. Orazi, C. Cicero, U. Zammit, Appl. Phys **123**, 317 (2017). https://doi.org/10.1007/s00339-017-0958-6
27. F. Mercuri, N. Orazi, A. Zammit, A. Giuffredi, C.S. Salerno, C. Cicero, S. Paoloni, J. Archaeol. Sci. Rep. **14**, 199–207 (2017). https://doi.org/10.1016/j.jasrep.2017.05.051
28. N. Orazi, F. Mercuri, U. Zammit, S. Paoloni, M. Marinelli, A. Giuffredi, C.S. Salerno, Stud. Conserv. **61**, 236–244 (2016)
29. F. Mercuri, N. Orazi, S. Paoloni, C. Cicero, U. Zammit, Appl. Sci. **7**, 2017 (1010). https://doi.org/10.3390/app7101010
30. S. Paoloni, F. Mercuri, U. Zammit, J. Chem. Phys. **145**, 124506 (2016)
31. M. Marinelli, F. Mercuri, S. Foglietta, U. Zammit, F. Scudieri, Phys. Rev. E **54**, 1604 (1996)